

THERMODYNAMICALLY AND ENVIRONMENTALLY EFFICIENT OFFSHORE GAS-TO-WIRE FROM CO₂-RICH NATURAL GAS WITH CARBON CAPTURE

Acceptance date: 01/12/2023

Alessandra de Carvalho Reis

Escola de Química, Federal University of Rio de Janeiro, CT, E, Ilha do Fundão, Rio de Janeiro, Brazil

Ofélia de Queiroz Fernandes Araújo

Escola de Química, Federal University of Rio de Janeiro, CT, E, Ilha do Fundão, Rio de Janeiro, Brazil

José Luiz de Medeiros

Escola de Química, Federal University of Rio de Janeiro, CT, E, Ilha do Fundão, Rio de Janeiro, Brazil

ABSTRACT: Increase in power generation from natural gas is predicted for the next decades, due to expansion of proved reserves and energy demand. In the Brazilian Pre-Salt offshore basin, oil reserves have a high gas-oil ratio with CO₂-rich associated gas. To bring such a gas to market demands the use of high-depth long-distance subsea pipelines making Gas-to-Pipe expensive. Gas-to-Wire instead of Gas-to-Pipe is a more suitable solution since it is easier to transport electricity than gas through long subsea distances. This work investigates the implementation of environment-friendly and thermodynamically efficient Gas-to-

Wire for CO₂-rich NG (CO₂≈44%*mol*) from high-depth offshore oil-&-gas fields. The process comprises natural gas combined-cycles, exhaust-gas recycle to reduce volume and increase CO₂ content of flue-gas, CO₂ post-combustion capture with aqueous-monoethanolamine for flue-gas decarbonation, and CO₂ dehydration with triethylene-glycol for exportation as enhanced oil recovery agent. The overall process exports 534.4 MW of low-emission net power. Second Law analysis reveals that the overall thermodynamic efficiency is 33.35%. Lost-work analysis showed that the greatest sink of power destruction lies in the gas-combined-cycle sub-system (80.7% lost-work), followed by the post-combustion capture plant (14.0% lost-work).

KEYWORDS: exhaust-gas recycle, gas-to-wire, natural gas combined-cycle, post-combustion carbon capture, second law analysis, thermodynamic analysis.

Nomenclature

$\dot{E}E$	Electricity (MW)
F_i	Flowrate of i^{th} feed-stream (kmol/s)
\bar{H}	Molar enthalpy (MJ/kmol)
N_f	Number of feed-streams (inputs)
N_p	Number of product-streams (outputs)
P	Pressure (bar)
P_i	Flowrate of i^{th} product-stream (kmol/s)
\dot{Q}, \bar{S}	Heat duty (MW), Molar entropy (MJ/K.kmol)
T, W	Temperature (K), Power (MW)
Greeks	
η	Thermodynamic efficiency (%)
Superscripts	
CW, Eq, LPS	Cooling-water, Equivalent, Low-pressure steam

1. INTRODUCTION

Despite the growing renewable energy utilization, fossil fuels still dominate the global energy matrix. Large growth in power generation from natural gas is anticipated for the incoming decades, due to expanding natural gas (NG) reserves and because NG is the cleanest fossil fuel (Neseli *et al.*, 2015).

According to Arinelli *et al.* (2017), in the Brazilian Pre-Salt offshore basin, deep-water oil reserves have a high gas-oil ratio with CO₂-rich associated gas (CO₂ ≈ 44% mol). To bring such a NG to market demands high-depth long-distance subsea pipelines entailing high investment despite the low-quality gas. In this scenario, Gas-to-Wire (GTW), instead of Gas-to-Pipe, is competitive since it is easier to transport electricity than gas through long subsea distances. In this context, floating Gas-to-Wire plants located nearby the offshore gas field convert the produced gas directly into electricity via NG combined-cycles (NGCC) for higher efficiency and the electricity is exported through High-Voltage Direct-Current (HVDC) cables for lower power losses (Watanabe *et al.*, 2006). Considering the climate-change conjuncture, Gas-to-Wire must include carbon capture and storage (CCS) to decrease the carbon-footprint of power generation (Zhou *et al.*, 2018). For GTW over offshore deep-water oil-&-gas fields, CCS must comprehend: (i) exhaust-gas recycle (EGR) to increase flue-gas CO₂ content and to decrease flue-gas volume both lowering CCS costs; (ii) post-combustion carbon capture from CO₂-rich flue-gas via benchmark absorption in aqueous-monoethanolamine (aqueous-MEA); i.e., the PCC-MEA plant; (iii) CO₂ compression; (iv) high-pressure CO₂ dehydration in a CO₂ Dehydration Unit (CDU) for low water content (≈200 ppm-mol) avoiding CO₂ hydrates; and (v) dense CO₂ injection in the oil-&-gas field for

enhanced oil recovery (EOR) accomplishing two objectives: CO₂ storage while improving oil production (Roussanaly *et al.*, 2019). Offshore GTW for CO₂-rich NG with EGR, CCS and CDU is written here as GTW-EGR-CCS-CDU.

There is a clear literature gap regarding GTW-EGR-CCS-CDU and its Thermodynamic Analysis (Second Law Analysis), thanks to the following cumulative process extreme particularities: CO₂-rich NG fuel-gas, EGR and CDU as process intensifiers. To fill this gap, the present work investigates the implementation and thermodynamic performance of GTW-EGR-CCS-CDU firing CO₂-rich NG from offshore deep-water oil-&-gas fields, simultaneously identifying the power destruction sinks and quantifying Lost-Work of the overall system and its sub-systems in order to pinpoint process components that should be upgraded for better thermodynamic efficiency.

2. METHODS

Offshore GTW-EGR-CCS-CDU firing CO₂-rich NG and exporting power and CO₂-to-EOR was designed and simulated in Aspen-HYSYS for technical and thermodynamic evaluations. The necessary theoretical frameworks follow.

2.1. PROCESS SUB-SYSTEMS

Figure 1 displays a block-diagram defining GTW-EGR-CCS-CDU sub-systems, while Table 1 depicts simulation and design assumptions. The skeleton of the medium-capacity ($\approx 600MW$) offshore GTW-EGR-CCS-CDU comprises: (i) NGCC Plant; (ii) Direct-Contact Column (DCC) for flue-gas cooling; (iii) low-pressure PCC-MEA for CO₂ capture; (iv) 1st CO₂ Compression Unit (CU-1); (v) CO₂ dehydration via high-pressure absorption with triethylene-glycol (TEG) for water removal from the CO₂-to-EOR stream (CDU-TEG); (vi) Stripping-Gas Unit (SGU) that adjusts the stripping-gas to the CDU-TEG reboiler; (vii) CO₂ pumping plant (CU-2) that dispatches CO₂-to-EOR; and (viii) EGR structure.

Table 1 - Simulation assumptions.

Item	Assumption
A1	Thermodynamic Models Gas-Streams: Peng-Robinson Equation-of-State; Rankine-Cycle: ASME Steam-Table; PCC-MEA: HYSYS Acid-Gas Package; CDU-TEG: HYSYS Glycol-Package
A2	Raw CO ₂ -Rich NG $6.5 \text{ MMSm}^3/\text{d}$; $T=40^\circ\text{C}$; $P=25 \text{ bar}$; $\text{CH}_4=49.82\% \text{ mol}$, $\text{CO}_2=43.84\% \text{ mol}$, $\text{C}_2\text{H}_6=2.99\% \text{ mol}$, $\text{C}_3\text{H}_8=1.99\% \text{ mol}$, $i\text{C}_4\text{H}_{10}=0.3\% \text{ mol}$, $\text{C}_4\text{H}_{10}=0.2\% \text{ mol}$, $i\text{C}_5\text{H}_{12}=0.2\% \text{ mol}$, $\text{C}_5\text{H}_{12}=0.1\% \text{ mol}$, $\text{C}_6\text{H}_{14}=0.1\% \text{ mol}$, $\text{C}_7\text{H}_{16}=0.05\% \text{ mol}$, $\text{C}_8\text{H}_{18}=0.03\% \text{ mol}$, $\text{C}_9\text{H}_{20}=0.01\% \text{ mol}$, $\text{C}_{10}\text{H}_{22}=0.01\% \text{ mol}$, $\text{H}_2\text{O}=0.36\% \text{ mol}$
A3	Air $T=25^\circ\text{C}$; $P=1.013 \text{ bar}$; $\text{N}_2=77.14\% \text{ mol}$; $\text{O}_2=20.51\% \text{ mol}$; $\text{H}_2\text{O}=2.35\% \text{ mol}$
A4	Gas-Turbine Aero-Derivative GE LM2500+G4; Efficiency ^{LHV} =36.5%; $P^{\text{Inlet}}=23 \text{ bar}$; Air-Ratio=6.2 mol/mol; $T^{\text{Flue-Gas}}=549^\circ\text{C}$.
A5	Steam-Turbine HPS: $P^{\text{Inlet}}=24 \text{ bar}$; $P^{\text{Outlet}}=0.12 \text{ bar}$; $T^{\text{Inlet}}=524^\circ\text{C}$; Outlet-Quality=98.1%.
A6	HRS $\Delta P^{\text{Flue-Gas}}=0.025 \text{ bar}$; $\Delta P^{\text{Steam}}=0.05 \text{ bar}$; $\Delta T^{\text{Approach}}=25^\circ\text{C}$.
A7	LPS $P^{\text{LPS}}=3 \text{ bar}$, $T^{\text{LPS}}=133.5^\circ\text{C}$.
A8	DCC Stages ^{Theoretical} =10; $P^{\text{Top}}=1.053 \text{ bar}$; $T^{\text{Top-Flue-Gas}}=40^\circ\text{C}$.
A9	PCC-MEA Absorber: Stages ^{Theoretical} =40; $P^{\text{Top}}=1.013 \text{ bar}$; $T^{\text{Inlet-Top}}=40^\circ\text{C}$; Capture=90%; Stripper: Stages ^{Theoretical} =10; $P^{\text{Top}}=1.013 \text{ bar}$; $T^{\text{Top}}=40^\circ\text{C}$; $T^{\text{Reboiler}}=103^\circ\text{C}$; Lean-MEA: $\text{H}_2\text{O}=63.3\% \text{ w/w}$, $\text{MEA}=31.6\% \text{ w/w}$, $\text{CO}_2=5.1\% \text{ w/w}$; Capture-Ratio: $\text{CR} \gg 14 \text{ kg}^{\text{Solvent}}/\text{kg}^{\text{CO}_2}$; Stripping Heat-Ratio: $\text{HR} \gg 225 \text{ kJ/mol}^{\text{CO}_2}$
A10	CDU-TEG Absorber: Stages ^{Theoretical} =15; $P=50 \text{ bar}$; $T^{\text{Inlet}}=35^\circ\text{C}$; Solvent: TEG=98.5% w/w; Stripper: Stages ^{Theoretical} =10; $P^{\text{Top}}=1.013 \text{ bar}$; $T^{\text{Top}}=40^\circ\text{C}$; $T^{\text{Reboiler}}=128^\circ\text{C}$;
A11	Compressors Stage Compression-Ratio=2.85; Intercoolers: $T^{\text{Gas-Outlet}}=35^\circ\text{C}$; $\Delta T^{\text{Approach}}=5^\circ\text{C}$; $\Delta P=0.5 \text{ bar}$.
A12	CO ₂ -to-EOR $T=35^\circ\text{C}$; $P=300 \text{ bar}$; Purity: $\text{CO}_2 \geq 99.9\% \text{ mol}$
A13	Cooling-Water CW: $T^{\text{Inlet}}=30^\circ\text{C}$; $T^{\text{Outlet}}=45^\circ\text{C}$; $P^{\text{Inlet}}=4 \text{ bar}$; $P^{\text{Outlet}}=3.5 \text{ bar}$.
A14	Exchangers $\Delta T^{\text{Approach}}=10^\circ\text{C}$ (gas-gas, liq-liq); $\Delta T^{\text{Approach}}=5^\circ\text{C}$ (gas-liq); $\Delta P=0.5 \text{ bar}$.
A15	Adiabatic Efficiencies $\eta^{\text{Pumps}}=\eta^{\text{Compressors}}=\eta^{\text{Steam-Turbine}}=75\%$; Gas-Turbines: $\eta^{\text{Air-Compressor}}=87\%$, $\eta^{\text{Expander}}=85.4\%$.
A16	Steam Production Priority: $\text{LPS}^{\text{PCC-MEA}}+\text{LPS}^{\text{CDU-TEG}}$; Surplus: $\text{HPS}^{\text{Rankine-Cycle}}$

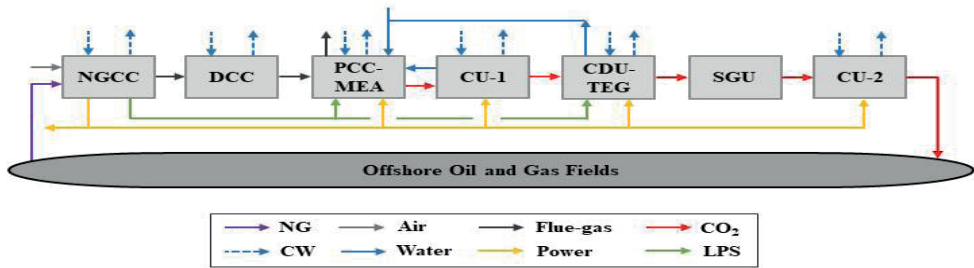


Figure 1 - Process sub-systems (NGCC=NG-Combined-Cycle, DCC=Direct-Contact-Column, PCC-MEA=Post-Combustion Capture with Aqueous-MEA, CU=CO₂-Compression-Unit, CDU-TEG=CO₂-Dehydration-TEG-Unit, SGU=Stripping-Gas-Unit, EGR=Exhaust-Gas-Recycle).

2.1.1. NGCC Plant

NGCC Plant comprehends five parallel NGCC elements for $\approx 600\text{MW}$ total electricity generation. Each NGCC element (Figure 2) has four gas-turbines connected to one Heat-Recovery Steam-Generator (HRSG) which heats the steam-cycle of the NGCC element (Rankine-Cycle). Aero-derivative gas-turbines (Table 1) are suitable for offshore rigs due to high power-to-weight ratio and low footprint (GE, 2019). Gas-turbines burn raw CO₂-rich NG (CO₂ $\approx 44\%$ mol) without any conditioning. The resulting flue-gas feeds the HRSG at $T=549^\circ\text{C}$ (GE, 2021) generating high-pressure superheated steam (HPS) ($T=524^\circ\text{C}$, $P=24\text{bar}$) and low-pressure steam (LPS) ($T=133.5^\circ\text{C}$, $P=3\text{bar}$). HPS expands in the steam-turbine to $P=0.12\text{bar}$ and is cooled down in the sub-atmospheric condenser with cooling-water (CW) returning as condensate to HRSG at $T=45^\circ\text{C}$. LPS heats PCC-MEA and CDU-TEG reboilers, consequently the steam-cycle power is limited by LPS demand.

Gas-turbine model in HYSYS consists of: (i) adiabatic single-stage air compressor; (ii) combustion-chamber modeled as adiabatic conversion reactor; and (iii) adiabatic expander. This model was calibrated to factory settings by adjusting adiabatic efficiencies of its air compressor and expander. Air is supplied at stoichiometric proportion for complete NG combustion. To limit combustion temperature to factory constraints, stoichiometric air is mixed with Exhaust-Gas Recycle (EGR). Recycled flue-gas is withdrawn after the DCC cooler and before the PCC-MEA and its flowrate was adjusted to match recommended flue-gas temperature at the expander outlet ($T=549^\circ\text{C}$).

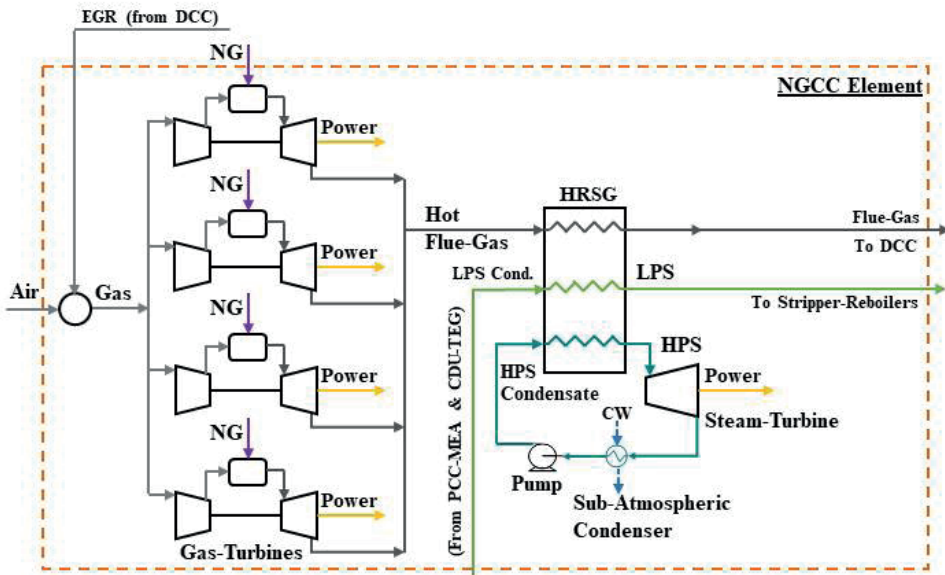


Figure 2 - NGCC Element (EGR=Exhaust-Gas-Recycle, HRSG=Heat-Recovery Steam-Generator, LPS=Low-Pressure-Steam, HPS=High-Pressure-Steam, CW=Cooling-Water, Direct-Contact-Column, PCC-MEA=Aqueous-MEA-Post-Combustion-Capture, CDU-TEG=CO₂-Dehydration-TEG-Unit).

2.1.2. Direct-Contact Column and Post-Combustion Capture with Aqueous-MEA

Flue-gas that leaves HRSG from the five NGCC elements is cooled down to 40°C and is water-saturated through direct-contact with CW ($T=30^{\circ}\text{C}$) in the Direct-Contact Column (DCC). The cooled flue-gas is divided: around 50% returns as EGR to the gas-turbine air feed to abate flame temperature; and the rest is sent to PCC-MEA for decarbonation with aqueous-MEA ($\text{MEA}\approx 30\%w/w$). Flue-gas is split into four smaller feeds (Figure 3) to improve capture-efficiency (Oh *et al.*, 2016). LPS ($P=3\text{bar}$, $T=133.5^{\circ}\text{C}$) heats the reboiler ($T=103^{\circ}\text{C}$) of the atmospheric PCC-MEA stripper. The stripper condenser operates in total reflux (i.e., 100% condensate reflux) and releases water-saturated CO₂ ($P=1\text{atm}$) through its vent. In order to keep CO₂ imprisoned in the CO₂-loop between PCC-MEA and CDU-TEG, all condensed carbonated waters ($T=35^{\circ}\text{C}$) from CU-1 knock-out vessels and from the TEG stripper condenser ($T=40^{\circ}\text{C}$) are recycled to tray#1 of the PCC-MEA stripper, while Wet-CO₂ from TEG stripper condenser vent ($T=40^{\circ}\text{C}$) is recycled to tray#10. These recycles reduce make-up water and condenser duty, and avoid CO₂ emissions from CU-1 and CDU-TEG. A pump recirculates Lean-MEA to PCC-MEA absorber after receiving make-up water. PCC-MEA is designed to capture 90% of CO₂ in the flue-gas under two key ratios that define solvent recirculation and stripper duty: the Capture-Ratio ($\text{CR}\approx 14\text{kg}^{\text{Solvent}}/\text{kg}^{\text{CO}_2}$) as the ratio of Lean-MEA to captured CO₂ and the stripper Heat-Ratio ($\text{HR}\approx 225\text{kJ}/\text{mol}^{\text{CO}_2}$). DCC and PCC-MEA sub-systems are shown in Figure 3.

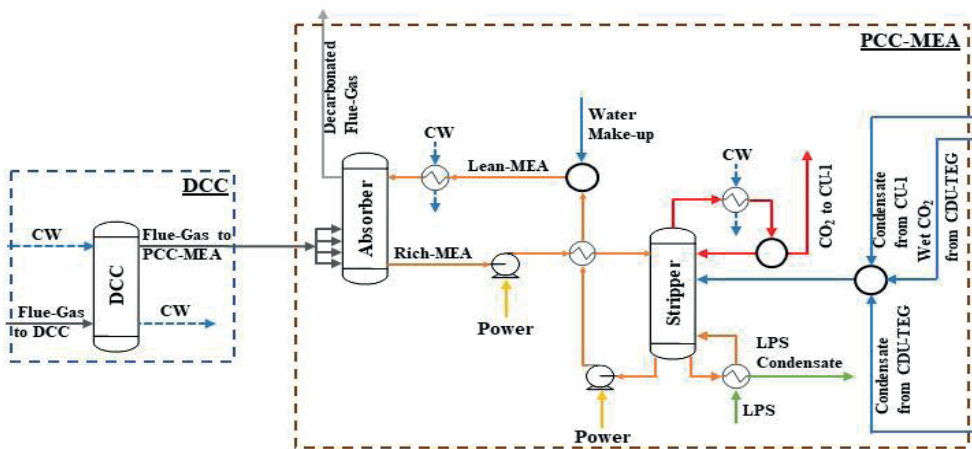


Figure 3 - Direct-Contact Column (DCC) and Aqueous-MEA-Post-Combustion-Capture (PCC-MEA) (LPS=Low-Pressure-Steam, CW=Cooling-Water, CDU-TEG=CO₂-Dehydration-TEG-Unit, CU=CO₂-Compression-Unit).

2.1.3. CO₂ Compression Units, CO₂ Dehydration Unit and Stripping-Gas Unit

CU-1 (Figure 4) is a 4-staged intercooled compression train (*stage-compression-ratio=2.85*) to raise the CO₂ pressure to 50 bar for CO₂ dehydration. The CO₂-to-CDU-TEG stream (*≈2700 ppm-mol H₂O*) and TEG solvent (*98.5%w/w TEG*) feed the 15-staged TEG-absorber of CDU-TEG producing Dry-CO₂ to SGU (*≈200ppm-mol H₂O*) at the top and rich-TEG (*H₂O≈60%mol*) at the bottom. TEG is regenerated in the 10-staged TEG-stripper, which produces Lean-TEG as bottoms (*T=128°C*), and vapor Wet-CO₂ and carbonated liquid water top distillates in the partial condenser. Water and Wet-CO₂ distillates are recycled to PCC-MEA. SGU is a small unit that adjusts the stripping-gas (*1% of Dry-CO₂*) in order to keep TEG-stripper reboiler temperature below 140°C. The remaining Dry-CO₂ is forwarded to CU-2, to achieve EOR pipeline pressure (*P=300bar*).

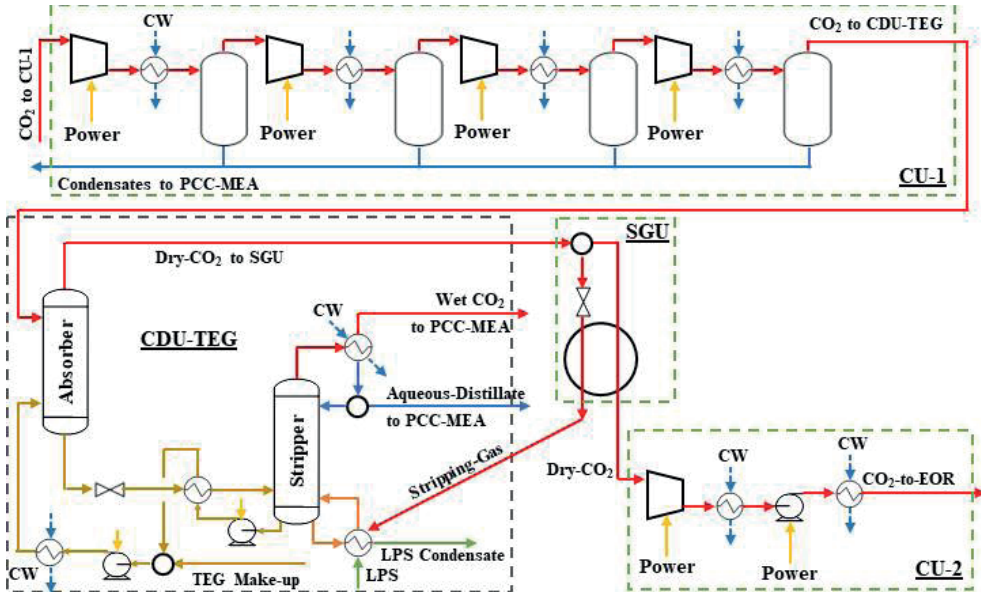


Figure 4 - Compression Units (CU1/CU2), CO₂-Dehydration-TEG-Unit (CDU-TEG) and Stripping-Gas-Unit (SGU) (CW=Cooling-Water, LPS=Low-Pressure-Steam, PCC-MEA=Aqueous-MEA-Post-Combustion-Capture, EOR=Enhanced Oil Recovery).

2.2. THERMODYNAMIC ANALYSIS OF PROCESSES

Thermodynamic analysis is effective to reveal resource degradation through processes. Steady-state Offshore GTW-EGR-CCS-CDU and its sub-systems are assessed via the Second Law analysis of processes. For 2nd Law analysis, systems and their sub-systems are previously classified as either power-consuming or power-producing systems. Figure 5 displays a steady-state open-system for thermodynamic analysis with several feed/product streams (green/blue arrows, respectively) interacting with an infinite isothermal heat reservoir R_0 at temperature T_0 . The overall system and its sub-systems can be power-producing ($\dot{W} > 0$) or power-consuming ($\dot{W} < 0$), but can only have thermal interactions with R_0 either absorbing ($\dot{Q} > 0$) or rejecting ($\dot{Q} < 0$) heat. $F_n, \bar{H}_{F_n}, \bar{S}_{F_n}$ respectively represent molar flowrate ($kmol/s$), enthalpy ($MJ/kmol$) and entropy ($MJ/kmol.K$) of the n^{th} feed-stream ($n=1..Nf$), while $P_n, \bar{H}_{P_n}, \bar{S}_{P_n}$ are analogous for the n^{th} product-stream ($n=1..Np$).

2.2.1. Maximum Power

Eq. (1) and Eq. (2) represent the First Law of Thermodynamics applied to the steady-state Open-System (Figure 5). The System Maximum Power (Maximum Work) \dot{W}^{MAX} is calculated via the 2nd Law at reversible conditions using Eq. (3), Eq. (4), Eq. (5) and Eq. (6), where Eq. (4) represents the Universe entropy balance at reversible conditions and $\dot{S}^{UNIV^{REV}}$ is the Universe entropy-creation rate at reversible conditions. Eq. (5) results from Eq. (2), under reversibility, and Eq. (6) derives from Eq. (4). Thus, \dot{W}^{MAX} is given by Eq. (7)

or Eq. (8). For Power-Consuming Systems (e.g., PCC-MEA, CU-1, CU-2 and CDU-TEG) Eq. (8) gives negative \dot{W}^{MAX} , while for Power-Producing systems (e.g., NGCC Plant, DCC and SGU) Eq. (8) gives positive \dot{W}^{MAX} .

$$\sum_{i=1}^{Nf} F_i \bar{H}_{F_i} + \dot{Q} - \dot{W} = \sum_{i=1}^{Np} P_i \bar{H}_{P_i} \quad (1)$$

$$\dot{W} = - \left(\sum_{i=1}^{Np} P_i \bar{H}_{P_i} - \sum_{i=1}^{Nf} F_i \bar{H}_{F_i} \right) + \dot{Q} \quad (2)$$

$$\dot{W} = \dot{W}^{MAX}, \quad \dot{Q} = \dot{Q}^{REV} \quad (3)$$

$$\sum_{i=1}^{Np} P_i \bar{S}_{P_i} - \sum_{i=1}^{Nf} F_i \bar{S}_{F_i} - \frac{\dot{Q}^{REV}}{T_0} = \dot{S}^{UNIV^{REV}} = 0 \quad (4)$$

$$\dot{W}^{MAX} = - \left(\sum_{i=1}^{Np} P_i \bar{H}_{P_i} - \sum_{i=1}^{Nf} F_i \bar{H}_{F_i} \right) + \dot{Q}^{REV} \quad (5)$$

$$\dot{Q}^{REV} = T_0 \left(\sum_{i=1}^{Np} P_i \bar{S}_{P_i} - \sum_{i=1}^{Nf} F_i \bar{S}_{F_i} \right) \quad (6)$$

$$\dot{W}^{MAX} = - \left(\sum_{i=1}^{Np} P_i \bar{H}_{P_i} - \sum_{i=1}^{Nf} F_i \bar{H}_{F_i} \right) + T_0 \left(\sum_{i=1}^{Np} P_i \bar{S}_{P_i} - \sum_{i=1}^{Nf} F_i \bar{S}_{F_i} \right) \quad (7)$$

$$\dot{W}^{MAX} = - \left(\sum_{i=1}^{Np} P_i (\bar{H}_{P_i} - T_0 \bar{S}_{P_i}) - \sum_{i=1}^{Nf} F_i (\bar{H}_{F_i} - T_0 \bar{S}_{F_i}) \right) \quad (8)$$

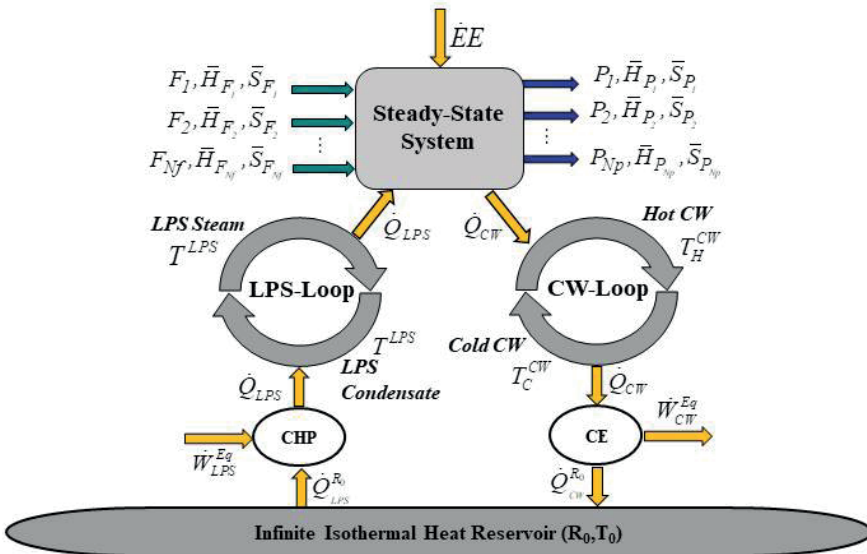


Figure 5 - Equivalent power for power-consuming System (blue-arrows=product-streams, green-arrows=feed-streams): imports electricity (\dot{E}), exports equivalent power via CW-Loop (\dot{W}_{CW}^{Eq}) and imports equivalent power via LPS-Loop (\dot{W}_{LPS}^{Eq}) (CW=Cooling-Water, LPS=Low-Pressure-Steam, CHP=Carnot-Heat-Pump, CE=Carnot-Engine).

2.2.2. Equivalent Power

Equivalent power \dot{W}^{Eq} is always-positive for “regular” systems, but can be negative for “lawless” systems like a theoretically power-producing system (i.e., spontaneous system) that consumes power (e.g., CW-Tower). \dot{W}^{Eq} is the thermodynamic power equivalence of electricity consumption (production) and utility consumption (production). For instance, LPS consumption (production) is equivalent to \dot{W}^{Eq} consumption (production), while CW consumption is always equivalent to \dot{W}^{Eq} production. Offshore GTW-EGR-CCS-CDU uses three kinds of utilities: (i) CW with flowrate J^{CW} (kmol/s), isobaric heat capacity \bar{C}_P^{CW} (MJ/kmol.K) and hot/cold temperatures T_H^{CW} (K), T_C^{CW} (K); (ii) LPS with flowrate J^{LPS} (kmol/s), vaporization-enthalpy $\Delta\bar{H}_{LPS}^{VAP}$ (MJ/kmol) and temperature T^{LPS} (K); and (iii) Electricity $\dot{E}E$ (MW). \bar{C}_P^{CW} and $\Delta\bar{H}_{LPS}^{VAP}$ are assumed constant considering CW and LPS narrow temperature ranges.

Equivalent Power is related to electricity consumption/production ($\dot{E}E$) and equivalent power effects associated to thermal utilities consumption/production (Carminati *et al.*, 2020). Heat-Power equivalences are settled through reversible heat-engines with maximum heat-work conversion yield; namely, the Carnot Engine (CE) and the Carnot Heat-Pump (CHP) (Milão *et al.*, 2021). CE absorbs heat from a hot source, exports power and rejects heat to a colder source, while CHP imports power, absorbs heat from a cold source and rejects heat to a hotter one. Figure 5 shows a Power-Consuming System with the following utility effects: absorbs $\dot{E}E$, rejects heat \dot{Q}_{CW} to CW-Loop (exports power \dot{W}_{CW}^{Eq}) and absorbs heat \dot{Q}_{LPS} from LPS-Loop (imports power \dot{W}_{LPS}^{Eq}). In Figure 5, CW-Loop and LPS-Loop are external to the System, R_o is always a cold heat reservoir (cold source), and \dot{W}_{CW}^{Eq} , \dot{Q}_{CW} , \dot{W}_{LPS}^{Eq} , \dot{Q}_{LPS} are always positive. It is easy to construct an analogous version of Figure 5 for a Power-Producing System (i.e., electricity and LPS are exported and CW is imported).

The steady-state Power-Consuming System (Figure 5) rejects heat \dot{Q}_{CW} to cold-CW producing hot-CW, which is restored to cold-CW via a CW-Loop using CE that exports power \dot{W}_{CW}^{Eq} and rejects heat \dot{Q}_{CW}^R to R_o . Analogously, the Power-Consuming System absorbs heat \dot{Q}_{LPS} from LPS becoming LPS-Condensate, which is restored to LPS via a LPS-Loop using CHP that imports power \dot{W}_{LPS}^{Eq} and absorbs heat \dot{Q}_{LPS}^R from R_o . \dot{W}_{CW}^{Eq} is given by Eq. (10) using Eq. (9a), Eq. (9b) and CE entropy conservation in Eq. (9c). Accordingly, is given by Eq. (12) using Eq. (11a), Eq. (11b) and CHP entropy conservation in Eq. (11c). Eq. (12) also works for \dot{W}_{LPS}^{Eq} in Power-Producing Systems, but LPS-Loop rotates counter-clockwise, CHP is replaced by CE, and all effects are reversed.

$$\dot{W}_{CW}^{Eq} = \dot{Q}_{CW} - \dot{Q}_{CW}^R \quad (9a)$$

$$\dot{Q}_{CW} = J^{CW} \bar{C}_P^{CW} (T_H^{CW} - T_C^{CW}) \quad (9b)$$

$$\frac{\dot{Q}_{CW}^{R_0}}{T_0} + J^{CW} \bar{C}_P^{CW} \ln \left(\frac{T_C^{CW}}{T_H^{CW}} \right) = 0 \quad (9c)$$

$$\dot{W}_{CW}^{Eq} = J^{CW} \bar{C}_P^{CW} \left(T_H^{CW} - T_C^{CW} - T_0 \cdot \ln \left(\frac{T_H^{CW}}{T_C^{CW}} \right) \right) \quad (10)$$

$$\dot{W}_{LPS}^{Eq} = \dot{Q}_{LPS} - \dot{Q}_{LPS}^{R_0} \quad (11a)$$

$$\dot{Q}_{LPS} = J^{LPS} \Delta \bar{H}_{LPS}^{VAP} \quad (11b)$$

$$-\frac{\dot{Q}_{LPS}^{R_0}}{T_0} + J^{LPS} \frac{\Delta \bar{H}_{LPS}^{VAP}}{T^{LPS}} = 0 \quad (11c)$$

$$\dot{W}_{LPS}^{Eq} = J^{LPS} \Delta \bar{H}_{LPS}^{VAP} \left(1 - \frac{T_0}{T^{LPS}} \right) \quad (12)$$

Eq. (13a) calculates the Equivalent Power *consumed* by a Power-Consuming System that consumes $\dot{E}E$, CW and LPS. Analogously, Eq. (13b) gives the Equivalent Power *produced* by a Power-Producing System that exports $\dot{E}E$ and LPS (counter-clockwise LPS-Loop in Figure 5) and consumes CW. Substituting Eqs. (10) and (12) into Eqs. (13a) and (13b), Eq. (14a) and Eq. (14b) are respectively created, giving the Equivalent Power consumed by a Power-Consuming System and the Equivalent Power produced by a Power-Producing System.

$$\dot{W}^{Eq} = \dot{E}E + \dot{W}_{LPS}^{Eq} - \dot{W}_{CW}^{Eq} \quad \{ \text{Power-Consuming System} \} \quad (13a)$$

$$\dot{W}^{Eq} = \dot{E}E + \dot{W}_{LPS}^{Eq} + \dot{W}_{CW}^{Eq} \quad \{ \text{Power-Producing System} \} \quad (13b)$$

$$\dot{W}^{Eq} = \dot{E}E + J^{LPS} \Delta \bar{H}_{LPS}^{VAP} \left(1 - \frac{T_0}{T^{LPS}} \right) - J^{CW} \bar{C}_P^{CW} \left(T_H^{CW} - T_C^{CW} - T_0 \cdot \ln \left(\frac{T_H^{CW}}{T_C^{CW}} \right) \right) \quad (14a)$$

$$\dot{W}^{Eq} = \dot{E}E + J^{LPS} \Delta \bar{H}_{LPS}^{VAP} \left(1 - \frac{T_0}{T^{LPS}} \right) + J^{CW} \bar{C}_P^{CW} \left(T_H^{CW} - T_C^{CW} - T_0 \cdot \ln \left(\frac{T_H^{CW}}{T_C^{CW}} \right) \right) \quad (14b)$$

2.2.3. Thermodynamic Efficiency

Second Law Analysis obtains the Thermodynamic Efficiency and the Lost-Work (Lost-Power) of the System in order to calculate resource degradation. With \dot{W}^{MAX} (Eq. (8)) and \dot{W}^{Eq} (Eqs. (14a) and (14b)) the thermodynamic efficiencies of Power-Consuming Systems and of Power-Producing Systems are calculated by Eq. (15a) and Eq. (15b), respectively.

$$\eta\% = 100 \cdot (-\dot{W}^{MAX}) / \dot{W}^{Eq} \quad \{ \text{Power-Consuming System} \} \quad (15a)$$

$$\eta\% = 100 \cdot \dot{W}^{Eq} / \dot{W}^{MAX} \quad \{ \text{Power-Producing System} \} \quad (15b)$$

2.2.4. Lost-Work

Eq. (16a) and Eq. (16b) are naturally intuitive Lost-Work (Lost-Power) formulas for Power-Consuming Systems and Power-Producing Systems, respectively.

$$\dot{W}^{LOST} = \dot{W}^{Eq} - (-)\dot{W}^{MAX} \quad \{ \text{Power-Consuming System} \} \quad (16a)$$

$$\dot{W}^{LOST} = \dot{W}^{MAX} - \dot{W}^{Eq} \quad \{ \text{Power-Producing System} \} \quad (16b)$$

An alternative way to calculate Lost-Work can be derived from the 2nd Law formula Eq. (17a) that accounts for all Universe changes caused by System transitions, where \dot{S}^{UNIV} is the entropy-creation rate of the Universe due to the System operation. Hence, Eq. (17b) and Eq. (17c) are Lost-Work formulas generated by Eq. (17a) for Power-Consuming Systems and for Power-Producing Systems, respectively, where \dot{S}^{R_0} was replaced by Eq. (18a) and Eq. (18b), respectively for Power-Consuming Systems (Figure 5) and Power-Producing Systems.

$$\dot{W}^{LOST} = T_0 \dot{S}^{UNIV} = T_0 \left(\dot{S}^{R_0} + \sum_{i=1}^{Np} P_i \bar{S}_{P_i} - \sum_{i=1}^{Nf} F_i \bar{S}_{F_i} \right) \quad (17a)$$

$$\dot{W}^{LOST} = -J^{LPS} \Delta \bar{H}_{LPS}^{VAP} \left(\frac{T_0}{T^{LPS}} \right) + J^{CW} \bar{C}_P^{CW} T_0 \cdot \ln \left(\frac{T_H^{CW}}{T_C^{CW}} \right) + T_0 \left(\sum_{i=1}^{Np} P_i \bar{S}_{P_i} - \sum_{i=1}^{Nf} F_i \bar{S}_{F_i} \right) \quad (17b)$$

$$\dot{W}^{LOST} = J^{LPS} \Delta \bar{H}_{LPS}^{VAP} \left(\frac{T_0}{T^{LPS}} \right) + J^{CW} \bar{C}_P^{CW} T_0 \cdot \ln \left(\frac{T_H^{CW}}{T_C^{CW}} \right) + T_0 \left(\sum_{i=1}^{Np} P_i \bar{S}_{P_i} - \sum_{i=1}^{Nf} F_i \bar{S}_{F_i} \right) \quad (17c)$$

$$\dot{S}^{R_0} = \frac{\dot{Q}_{CW}^{R_0}}{T_0} - \frac{\dot{Q}_{LPS}^{R_0}}{T_0} = J^{CW} \bar{C}_P^{CW} \ln \left(\frac{T_H^{CW}}{T_C^{CW}} \right) - J^{LPS} \frac{\Delta \bar{H}_{LPS}^{VAP}}{T^{LPS}} \quad (18a)$$

$$\dot{S}^{R_0} = \frac{\dot{Q}_{CW}^{R_0}}{T_0} + \frac{\dot{Q}_{LPS}^{R_0}}{T_0} = J^{CW} \bar{C}_P^{CW} \ln \left(\frac{T_H^{CW}}{T_C^{CW}} \right) + J^{LPS} \frac{\Delta \bar{H}_{LPS}^{VAP}}{T^{LPS}} \quad (18b)$$

3. RESULTS AND DISCUSSION

Results from technical and thermodynamic analyses of the Offshore GTW-EGR-CSS-CDU follow and are discussed.

3.1. TECHNICAL PERFORMANCE

Table 2 summarizes the technical performance of Offshore GTW-EGR-CCS-CDU.

Table 2 - Technical results.

GTW-EGR-CCS-CDU			
Gross Power (MW)	599.3		
Power Demand (MW)	64.9		
Net Power (MW)	534.4		
CO ₂ Flue-Gas (t/h) (PCC-MEA Feed)	557.2		
CO ₂ Emissions (t/h) (Atmosphere)	59.6		
PCC-MEA Results			
CO ₂ Captured (t ^{CO2} /h)	497.6		
Capture-Ratio (kg ^{Solvent} /kg ^{CO2})	13.7		
Heat-Ratio (kJ/mol ^{CO2})	225		
Lean-Solvent (t/h)	6,814		
Absorber: T ^{Top} (°C) / T ^{Bottom} (°C)	62.2/61.9		
Flue-Gas Inlet (%molCO ₂)	17.3		
Decarbonated Flue-Gas (%molCO ₂)	1.8		
Stripper: T ^{Feed} (°C)/T ^{Top} (°C)/T ^{Bottom} (°C)	83/40/103		
Reboiler Duty (MW)	722		
CO ₂ to CU-1 (%molCO ₂)	92.7		
CDU-TEG Results			
Capture-Ratio (kg ^{TEG} /kg ^{H2O})	3.7		
Lean-Solvent (t/h)	2.1		
CO ₂ Inlet (ppm-mol H ₂ O)	2690.2		
CO ₂ Outlet (ppm-mol H ₂ O)	192.8		
Absorber: T ^{Top} (°C)/T ^{Bottom} (°C)	36.4/35.3		
Stripper: T ^{Feed} (°C)/T ^{Top} (°C)/T ^{Bottom} (°C)	62/40/128		
Reboiler Duty (MW)	0.6		
Utilities Demand	LPS (t/h)	CW (t/h)	Power (MW)
NGCC Plant	-	6,109	0.15
DCC	-	-	0.36
PCC-MEA	1,230	36,249	0.35
CU-1	-	3,894	50.9
CDU-TEG	1.1	22.4	0.00355
SGU	-	-	-
CU-2	-	2,324	13.17
Total	1,231	48,598	64.9

The NGCC Plant (with five parallel NGCC elements) of Offshore GTW-EGR-CCS-CDU generates 599.3MW of gross power ($\approx 92.4\%$ from gas-turbines) allowing 534.4MW of net exported power. Each gas-turbine fires ≈ 4.76 kg/s of fuel-gas producing ≈ 30 MW at 36.5% LHV-efficiency. Thanks to the EGR, each NGCC element produces 370.6 kg/s flue-gas at 16.5%mol CO₂. HRSG cools down the gas-turbine flue-gas from 549°C to 140°C, the

minimum temperature to maximize HPS generation allowing sufficient LPS for PCC-MEA and CDU-TEG.

PCC-MEA stripper requires 722.2MW of LPS and discharges 144.2kg/s of water-saturated CO_2 top product. CU-1 pressurizes the CO_2 stream up to 50bar and feeds CDU-TEG. CDU-TEG removes $\approx 93\%$ of water from CDU-TEG feed and produces 503.8 t/h of Dry- CO_2 ($\approx 193\text{ppm-mol H}_2\text{O}$). SGU sends 5.3 t/h of low-pressure Dry- CO_2 to the TEG stripper reboiler to keep its temperature below 140°C . TEG stripper reboiler demands 0.6MW of LPS. CU-2 exports 498.8 t/h of Dry- CO_2 ($P=300\text{bar}$, $T=35^\circ\text{C}$) to EOR. The power demand of Offshore GTW-EGR-CCS-CDU corresponds to 10.8% of its gross power. The greatest electricity consumers are CU-1 and CU-2 compressor trains, while the greatest LPS and CW consumer is PCC-MEA. CDU-TEG requires a small LPS flowrate because the flowrate of captured water from the CO_2 stream is a tiny one.

3.2. THERMODYNAMIC ANALYSIS

Thermodynamic analysis and Lost-Work analysis were performed for Offshore GTW-EGR-CCS-CDU overall-system and its sub-systems, namely: (i) NGCC Plant; (ii) DCC; (iii) PCC-MEA; (iv) CU-1; (v) CDU-TEG; (vi) SGU and (vii) CU-2. There is no sub-system left; i.e., the GTW-EGR-CCS-CDU is correctly partitioned among the above sub-systems, which entail that the respective sums of \dot{W}^{MAX} , \dot{W}^{Eq} and \dot{W}^{LOST} over sub-systems would give the same value of the overall-system which are calculated independently of the sub-systems. Confrontation of overall-system values with the respective sum over sub-systems configures a consistency check of the thermodynamic analysis. In practice, there is always some divergence between overall-system and the sums over sub-systems, such that divergences below 1% can be used to attest consistency of thermodynamic analysis.

3.2.1. Maximum Power, Equivalent Power and Thermodynamic Efficiency Results

Table 3 depicts thermodynamic efficiencies and other results of Second Law analysis of Offshore GTW-EGR-CCS-CDU and its sub-systems. Sub-systems PCC-MEA, CU-1, CDU-TEG and CU-2 are Power-Consuming Systems ($\dot{W}^{MAX} < 0$), thus Eq. (13a), Eq. (14a), Eq. (15a), Eq. (16a), Eq. (17b) and Eq. (18a) were used for $\dot{W}^{Eq}, \eta\%$, \dot{W}^{LOST} . On the other hand, the overall-system, NGCC Plant, DCC and SGU are Power-Producing Systems ($\dot{W}^{MAX} > 0$) and require Eq. (13b), Eq. (14b), Eq. (15b), Eq. (16b), Eq. (17c) and Eq. (18b) for $\dot{W}^{Eq}, \eta\%$, \dot{W}^{LOST} . The thermodynamic efficiency of overall Offshore GTW-EGR-CCS-CDU reaches 33.35% (Table 3).

The NGCC Plant is evidently a Power-Producing System due to its spontaneous transformations within the NGCC elements totaling a positive $\dot{W}^{MAX} = 1678.12\text{MW}$. The \dot{W}^{Eq} produced by each NGCC element is calculated as follows: $\dot{E}E$ produced as gas-

turbines+steam-turbine power minus the Rankine-Cycle pump power (Figure 2), added to \dot{W}_{CW}^{Eq} generated by Rankine-Cycle condenser, added to \dot{W}_{LPS}^{Eq} from HRSG LPS exportation. The thermodynamic efficiency of NGCC Plant reached 48.62%.

In DCC, CW should not be counted as utility ($\dot{W}_{CW}^{Eq} = 0$), since CW is a process stream suffering evaporation loss through DCC. Additionally, LPS was not consumed ($\dot{W}_{LPS}^{Eq} = 0$). Thus, only $\dot{E}E$ from the pump contributes (negatively) to \dot{W}^{Eq} . DCC \dot{W}^{Eq} is negative because it is a Power-Producing System performing spontaneous changes ($\dot{W}^{MAX} > 0$), but no power was produced at all and electricity was consumed.

Table 3 - Second Law Analysis and Lost-Work Validation.

Second Law Analysis						
Sub-System	\dot{W}^{MAX} (MW)	\dot{W}_{LPS}^{Eq} (MW)	\dot{W}_{CW}^{Eq} (MW)	$\dot{E}E$ (MW)	\dot{W}^{Eq} (MW)	$\eta\%$
NGCC Plant	1678.12	212.37	4.40	599.18	815.96	48.62%
DCC	26.31	-	-	-0.36	-0.36	-1.37%
PCC-MEA	-31.29	212.19	31.41	0.35	181.14	17.27%
CU-1	-28.41	-	2.81	50.90	48.09	59.09%
CDU-TEG	-0.00014	0.18	0.07	0.00355	0.12	0.12%
SGU	0.48	-	-	-	-	0.00%
CU-2	-4.88	-	1.68	13.17	11.49	42.49%
Overall System	1602.33	-	-	534.40	534.40	33.35%
Lost-Work and Lost-Work Validation						
Sub-System	\dot{W}^{LOST} (MW) [*]	\dot{W}^{LOST} (MW) [#]	$\Delta\dot{W}^{LOST}$ (%)			
NGCC Plant	862.16	860.66	0.17			
DCC	26.67	26.50	0.64			
PCC-MEA	149.85	149.03	0.55			
CU-1	19.67	19.74	-0.36			
CDU-TEG	0.1193	0.1189	0.34			
SGU	0.480	0.478	0.42			
CU-2	6.61	6.59	0.30			
Sum-Crosscheck	1065.56	1063.12	0.23			
Overall-System	1067.93	1061.74	0.58			

^{*}via Eqs. (16a)-(16b); [#]via Eqs. (17b)-(17c).

As any separation process, PCC-MEA is a Power-Consuming System since \dot{W}^{MAX} is negative due to CO₂ separation from flue-gas (-31.29 MW); i.e., PCC-MEA requires power consumption to work. PCC-MEA \dot{W}^{Eq} consumption is calculated as follows: $\dot{E}E$ consumed in solvent recirculation and water make-up pumps is added to \dot{W}_{LPS}^{Eq} consumed in PCC-MEA stripper reboiler, minus \dot{W}_{CW}^{Eq} exported as Hot-CW from PCC-MEA stripper condenser and from lean-MEA cooler. PCC-MEA thermodynamic efficiency is 17.27%.

CDU-TEG, another separation process, is too a Power-Consuming System ($\dot{W}^{MAX} = -0.00014MW$). The small \dot{W}^{MAX} derives from the small flowrate of water removed for CO₂ dehydration (from ≈ 2700 ppm-mol H₂O to ≈ 200 ppm-mol H₂O). CDU-TEG has $\dot{W}^{Eq} = 0.12MW$ calculated as follows: (i) $\dot{E}E$ consumed in TEG recirculation pumps is added to \dot{W}_{LPS}^{Eq} consumed through LPS consumption in stripper reboiler, minus \dot{W}_{CW}^{Eq} exported through Hot-CW from stripper condenser and from lean-TEG cooler. CDU-TEG thermodynamic efficiency is 0.12%.

SGU is another sub-system driven by spontaneities; i.e., it is a Power-Producing System ($\dot{W}^{MAX} = 0.48MW$). But its thermodynamic efficiency is 0% because $\dot{E}E$, \dot{W}_{LPS}^{Eq} and \dot{W}_{CW}^{Eq} are all zero.

CU-1 and CU-2 perform non-spontaneous (compression) changes and are evidently Power-Consuming Systems ($\dot{W}^{MAX} = -28.41MW$ and $\dot{W}^{MAX} = -4.88MW$). The respective \dot{W}^{Eq} is calculated as follows: $\dot{E}E$ consumed in compressors and pump is subtracted from \dot{W}_{CW}^{Eq} exported with Hot-CW from intercoolers. There is no LPS consumption ($\dot{W}_{LPS}^{Eq} = 0$). CU-1 and CU-2 thermodynamic efficiencies are 59.09% and 42.49%, respectively.

3.2.2. Lost-Work Results

Lost-Work reveals the power potential destroyed in GTW-EGR-CCS-CDU and its sub-systems due to irreversibility (spontaneity). Table 3 presents Lost-Work results and also proves the consistency of the present thermodynamic analysis by comparing Lost-Work values obtained via two thermodynamically independent ways: (i) via \dot{W}^{MAX} and \dot{W}^{Eq} in Eq. (16a) and Eq. (16b); and (ii) via $T_o \cdot \dot{S}^{UNIV}$ in Eq. (17b) and Eq. (17c) for Power-Consuming and Power-Producing Systems, respectively. Table 3 also demonstrates consistency crosscheck in the sum of Lost-Works over sub-systems which, theoretically, should equals the overall-system Lost-Work (divergences are smaller than 1%).

Figure 6 displays Sankey diagrams for \dot{W}^{MAX} , \dot{W}^{Eq} and \dot{W}^{LOST} flows for overall-system and its sub-systems. In Figure 6, \dot{W}^{LOST} is the sum over sub-systems of Lost-Works ("pink" flows), while $\Delta\dot{W}^{LOST}$ is the difference to overall-system Lost-Work (Table 3). For 1602.3.2MW of power availability (\dot{W}^{MAX}) in Offshore GTW-EGR-CCS-CDU 66.65% is lost due to irreversibility. NGCC Plant has the greatest $\Delta\dot{W}^{LOST}$ (832.2MW, 80.7%) due to highly spontaneous combustion reactions, followed by PCC-MEA (149.9MW, 14.0%), DCC (26.7MW, 2.5%), CU-1 (19.7MW, 1.8%), CU-2 (6.6MW, 0.6%), SGU (0.48MW, 0.04%), and CDU-TEG (0.1MW, 0.01%).

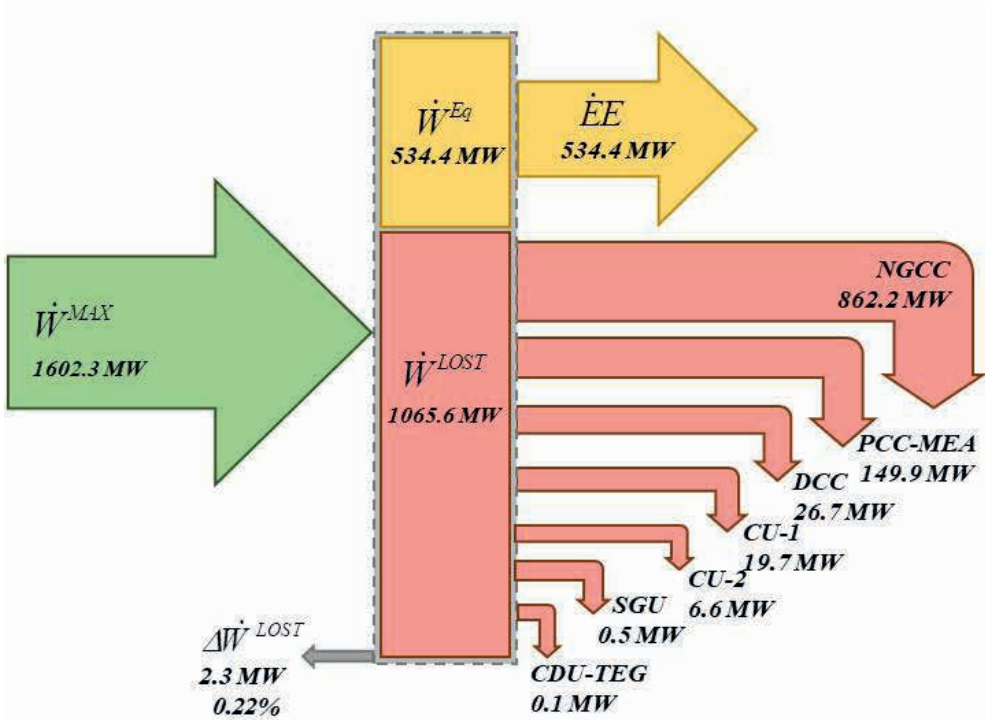


Figure 6 - Lost-Work Sankey diagram (\dot{E} =Electricity, \dot{W}^{MAX} =Maximum-Power, \dot{W}^{LOST} =Lost-Work, \dot{W}^{Eq} =Equivalent Power, NGCC=NG-Combined-Cycle, DCC=Direct-Contact-Column, PCC-MEA=Aqueous-MEA-Post-Combustion-Capture, CU=CO₂-Compression-Unit, CDU-TEG=CO₂-Dehydration-TEG-Unit, SGU=Stripping-Gas-Unit).

CONCLUSIONS

This work performed Technical and Thermodynamic Analyses of a conceptual Offshore GTW-EGR-CCS-CDU process firing $\approx 6.5 \text{ MMSm}^3/\text{d}$ of CO₂-rich NG (CO₂ $\approx 44\% \text{ mol}$), exporting low-emission electricity and dense CO₂ as EOR-Fluid for economic and environmental benefits. Offshore GTW-EGR-CCS-CDU exports 534.4MW of net power capturing $\approx 90\%$ of the flue-gas CO₂. CU-1 compresses the CO₂ stream up to 50bar in order to perform CO₂ dehydration in CDU-TEG. Offshore GTW-EGR-CCS-CDU is an intensified process, whose factors of intensification comprehend the Exhaust-Gas Recycle (EGR) and the high-pressure CO₂ dehydration in CDU-TEG which removes $\approx 93\%$ of water from the CO₂-to-EOR stream delivering a safe CO₂-to-EOR stream with $\approx 200 \text{ ppm-mol H}_2\text{O}$. By its turn, EGR is important whenever post-combustion capture is being used because it dismisses air excess (typically $\approx 100\%$) for gas-turbine flame temperature abatement, consequently reducing by $\approx 50\%$ the flue-gas volumetric flow and raising its CO₂ content from typical $\approx 8\% \text{ mol}$ (no EGR) to $\approx 17\% \text{ mol}$ (with EGR). These two consequences of EGR drastically reduce investment and manufacture cost of the PCC-MEA plant due to reductions of column diameter and height improving low-emission GTW profitability.

The 2nd Law analysis of Offshore GTW-EGR-CCS-CDU overall-system unveils a 33.35% thermodynamic efficiency with 66.65% of Lost-Work, whose greatest Lost-Work sink lies in the NGCC Plant sub-system (80.7% share), due to the highly spontaneous gas-turbine firing process. The second Lost-Work sink lies in PCC-MEA sub-system (14.0% share). Thus, the NGCC Plant and PCC-MEA are the main units of GTW-EGR-CCS-CDU that deserve upgrading in order to bring most benefits to GTW-EGR-CCS-CDU. The consistency of the thermodynamic analysis was established through Lost-Work sum-crosschecks and lateral checks using the alternative 2nd Law formula $T_o \cdot \dot{S}^{UNIV}$ for the Lost-Work (Table 3).

ACKNOWLEDGMENTS

Authors acknowledge financial support from Petrobras S/A (5850.0107386.18.9). JL de Medeiros and OQF Araújo also acknowledge support from CNPq-Brazil (313861/2020-0, 312328/2021-4).

REFERENCES

ARINELLI, L.O. *et al.* Offshore processing of CO₂ rich natural gas with supersonic separator versus conventional routes. **Journal of Natural Gas Science and Engineering**. v. 46, p. 199–221, 2017. DOI: 10.1016/j.jngse.2017.07.010.

CARMINATI, H.B. *et al.* Low-emission pre-combustion gas-to-wire via ionic-liquid [Bmim][NTf₂] absorption with high-pressure stripping. **Renewable and Sustainable Energy Reviews**. v. 131, 2020. DOI: 10.1016/j.rser.2020.109995.

GE Aeroderivative LM2500 Gas Turbine (50Hz): Fact Sheet. 2019. Available in: <https://www.ge.com/content/dam/gepower/global/en_US/documents/gas/gas-turbines/aero-products-specs/lm2500-50hz-fact-sheet-product-specifications.pdf>. (Accessed 02/09/2022).

GE. LM2500+G4 Marine Gas Turbine. 2021. Available in: <<https://www.geaviation.com/sites/default/files/datasheet-lm2500plusg4.pdf>>. (Accessed 02/09/2022).

MILÃO, R.F.D., ARAÚJO, O.Q.F., DE MEDEIROS, J.L. Second Law analysis of large-scale sugarcane-ethanol biorefineries with alternative distillation schemes: Bioenergy carbon capture scenario. **Renewable and Sustainable Energy Reviews**. v. 135, 2021. DOI: 10.1016/j.rser.2020.110181.

NESELI, M.A., OZGENER, O., OZGENER, L. Energy and exergy analysis of electricity generation from natural gas pressure reducing stations. **Energy Conversion and Management**. v. 93, p. 109–120, 2015. DOI: 10.1016/j.enconman.2015.01.011.

OH, S.Y. *et al.* Energy minimization of MEA-based CO₂ capture process. **Applied Energy**. v. 169, p. 353–362, 2016. DOI: 10.1016/j.apenergy.2016.02.046.

ROUSSANALY, S. *et al.* Offshore power generation with carbon capture and storage to decarbonize mainland electricity and offshore oil and gas installations: A techno-economic analysis. **Applied Energy**. v. 233–234, p. 478–494, 2019. DOI: 10.1016/j.apenergy.2018.10.020.

WATANABE, T. *et al.* Gas to Wire (GTW) system for developing small gas field and exploiting associated gas. International Oil and Gas Conference and Exhibition in China 2006 - Sustainable Growth for oil and Gas. v. 1, n. 2, p. 310–315, 2006. DOI: 10.2523/103746-ms.

ZHOU, D. *et al.* A long-term strategic plan of offshore CO₂ transport and storage in northern South China Sea for a low-carbon development in Guangdong province, China. **International Journal of Greenhouse Gas Control**. v. 70, p. 76–87, 2018. DOI: 10.1016/j.ijggc.2018.01.011.